Hanan F. Abd El-Halim et al. / Journal of Pharmacy Research 2012,5(11),5084-5092

Research Article
ISSN: 0974-6943

Available online through
www.jpronline.info

Cr(III), Mn(II), Fe(III), Co(II), Ni(II), Cu(II), Zn(II), Th(IV) and UO_2(II) Mixed Ligand Complexes of Lomefloxacin and Dl-Alanine. Preparation, Spectroscopic Characterization, Biological and Anticancer Activity

Hanan F. Abd El-Halim[1], Gehad G. Mohamed[*2], M.M.I. El-Dessouky[2], Walaa H. Mahmoud[2]

[1]*Pharmaceutical Chemistry Department, Faculty of Pharmacy, Misr International University, Cairo, Egypt.*

[2]*Chemistry Department, Faculty of Science, Cairo University, 12613, Giza, Egypt.*

Received on:23-07-2012; Revised on: 28-08-2012; Accepted on:12-09-2012

ABSTRACT

Mixed ligand transition metal complexes with general formula [M(LFX)(Ala)(H_2O)$_2$]Cl and [M(LFX)(Ala)(H_2O)m](X)n•yH_2O (LFX = lomefloxacin, Ala = alanine, M = Fe(III), Ni(II), Cu(II), X = Cl , m = 2, n = 1,2, y = 1-2), [M(LFX)(Ala)(H_2O)m](X)n (M = Cr(III), Co(II), Mn(II), Zn(II), X = Cl, n = 1-3, m = 2) and [M(LFX)(Ala)](X)n (M = UO_2(II), Th(IV), X = Cl or NO_3, n = 2, 3) have been synthesized and characterized using different spectroscopic tools, magnetic susceptibility, conductivity measurements and thermal analysis. The present results suggested that the lomefloxacin as bidentate coordinated with metal ions through carbonyl oxygen and carboxylate. The alanine as monodentate is coordinated with metal ions through the amino nitrogen atom and deprotonated carboxylate. LFX and its metal complexes were screened for their biological activity. Metal complexes exhibit higher antibacterial and antifungal than the free ligand. The anticancer activities against breast cancer cell line (MCF7) by using 100 µg / ml drug concentration were also tested. LFX and its metal complexes except Cr(III), Fe(III) and Th(IV) complexes were found to be very active against breast cancer cells with inhibition ratio values between 70-85.5 %.

Key words: Lomefloxacin, alanine, mixed ligand complexes, spectroscopic, biological activity, anticancer activity.

INTRODUCTION

Quinolones comprise a group of well-known antibacterial agents and the first members have been in clinical practice for over 40 years [1,2]. They are nowadays clinically the most successful synthetic antibacterial agents [2].Quinolones (quinolonecarboxylic acids or 4-quinolones) are synthetic antibacterial agents containing a 4-oxo-1,4-dihydroquinoline skeleton [3,4]. They can act as antibacterial drugs that effectively inhibit DNA replication and are commonly used as treatment for many infections [4,5]. They are very useful and helpful in daily clinical and veterinary practice for treatment of various infections, such as urinary tract infections, tissue infections, respiratory system infections and sexually transmitted diseases[6]. It is known that many pharmaceutical preparations containing metal ions, multi-mineral preparations or antacida may significantly reduce the oral absorption and bioavailability of the fluoroquinolones. Also the complexation of fluoroquinolones with metal ions has attracted considerable for the development of electroanalytical and spectrophotometric methods for determination of quinolones in pharmaceutical formulation[7–12] and to provide information about the action mechanism of the pharmaceutical compound [10–12].The probable mechanism of this interaction could be the chelation between the metal cation and the 3-carboxylate and 4-carbonyl groups [6,13,14]. Because of mediation in binding to the DNA-gyrase complex, the 3-carboxylate and 4-carbonyl groups of the fluoroquinolones are essential for the antimicrobial activity. It was confirmed that the strength of this ternary complex with DNA depends also on the concentration of magnesium ions, taking part in the formation of the complex [15].

The structures, the spectroscopic and the biological properties of diverse transition metal complexes with various quinolone antibacterial drugs have been thoroughly studied[16–26] in an attempt to examine the binding mode and possible synergetic effects. Here, we present the interaction of diverse transition metal ions with the second generation quinolone lomefloxacin and dl-alanine in order to study the mode of coordination and the biological properties of the resultant complexes. More specifically, the ternary complexes of lomefloxacin with Cr(III), Mn(II), Fe(III), Co(II), Ni(II), Cu(II), Zn(II), Th(IV) and UO_2(II) have been synthesized and characterized with elemental analysis, IR, UV–Vis, diffused reflectance, and 1HNMR spectroscopies, X-ray powder diffraction, conductivity, magnetic susceptibility and thermal analyses (TGA and DTA). The biological activity of the complexes has been evaluated by determining the minimum inhibitory concentration (MIC) against three microorganisms. The prepared complexes containing two different ligands were found to be quite stable.

***Corresponding author.**
Prof. Dr. Gehad G. Mohamed
Professor of Inorganic and Analytical Chemistry
Associate Editor of Journal Advanced Research (Cairo University)
Chemistry Department, Faculty of Science, Cairo University, Giza, Egypt

Experimental

MATERIALS AND METHODS

All chemicals were obtained from commercial sources and were used without further purifications ($CoCl_2$.6H_2O, $NiCl_2$.6H_2O, $CuCl_2$.2H_2O, $ZnCl_2$, $CrCl_3$.6H_2O, $FeCl_3$.6H_2O, $UO_2(NO_3)_2$.2H_2O and $ThCl_4$) fromRiedeal-Dehaenage. Lomefloxacin and alanine were obtained from BDH, methanol, ethanol and dimethylsulfoxide from Fluka.

Dimethylsulphoxide (DMSO) (was supplied from Sigma Chemical Co., St. Louis, Mo, and USA. It was used in cryopreservation of cells. RPMI-1640 medium (Sigma Chemical Co., St. Louis, Mo, and USA) is used. The medium was used for culturing and maintainance of the human tumor cell lines. The medium was supplied in a powder form. It was prepared as follows: 10.4 gm medium was weighed, mixed with 2 g sodium bicarbonate, completed to 1 L with distilled water and shacked carefully till complete dissolution. The medium was then sterilized by filtration in a Millipore bacterial filter (0.22 µm). The prepared medium was kept in a refrigerator (4 °C) and checked at regular intervals for contamination. Before use the medium was warmed at

37°C in a water bath and the supplemented with penicillin/streptomycin and FBS.

Sodium bicarbonate (Sigma Chemical Co., St. Louis, Mo, USA) was used for the preparation of RPMI-1640 medium. 0.05% isotonic Trypan blue solution (Sigma Chemical Co., St. Louis, Mo, USA) was prepared in normal saline and was used for viability counting. 10% Fetal Bovine Serum (FBS) (heat inactivated at 56 °C for 30 min), 100 units/ml Penicillin and 2 mg/ml Streptomycin were supplied from Sigma Chemical Co., St. Louis, Mo, USA and were used for the supplementation of RPMI-1640 medium prior to use. 0.025% (w/v) Trypsin (Sigma Chemical Co., St. Louis, Mo, USA) was used for the harvesting of cells. 1% (v/v) Acetic acid (Sigma Chemical Co., St. Louis, Mo, USA) was used for dissolving the unbound SRB dye. 0.4% Sulphorhodamine-B (SRB) (Sigma Chemical Co., St. Louis, Mo, USA) dissolved in 1 % acetic acid was used as a protein dye. A stock solution of trichloroacetic acid (TCA, 50%, Sigma Chemical Co., St. Louis, Mo, USA) was prepared and stored. 50 µl of the stock was added to 200 µl RPMI-1640 medium/well to yield a final concentration of 10 % used for protein precipitation. 100% isopropanol and 70 % ethanol were used. Tris base 10 mM (pH 10.5) was used for SRB dye solubilization. 121.1 gm of tris base was dissolved in 1000 ml of distilled water and pH was adjusted by HCl acid (2 M).

The I.R spectra in the range of 4000 – 400 cm^{-1} were recorded as potassium bromide disc on Perkin-Elmer FT-IR type 1650 spectrophotometer. UV-Visible spectra were measured in DMSO using Shimadzu UV-Visible recorder spectrophotometer UV-mini 1240. Elementalanalysis (C,H,N) was performed by the Microanalytical unit at Cairo University onCHNS-932 (LECO) Vario Elemental Analyzers. Determinations of metals were carried out using laboratory methods. Conductivity measurements were carried out at 25°C in DMF using Jenway 4010 conductivity meter. Melting point was determined using Stuart-Melting Point Apparatus. The magnetic susceptibility measurements were obtained using Balance Magnetic Susceptibility Model MsB-MK1 at 30°C. The solid reflectance spectra were measured on a Shimadzu 3101pc spectrophotometer. The molar magnetic susceptibility was measured on powdered samples using the Faraday method. The diamagnetic corrections were made by Pascal's constant and $Hg[Co(SCN)_4]$ was used as a calibrant. The ^1H NMR spectra were recorded using 300 MHz Varian-Oxford Mercury. The deuterated solvent used was dimethylsulphoxide (DMSO-d6) and the spectra extended from 0 to 15 ppm. The thermal analyses (TG, DTG and DTA) were carried out in dynamic nitrogen atmosphere (20 mL. min^{-1}) with a heating rate of 10 °C min^{-1} using Shimadzu TG-50H thermal analyzers. The X-ray powder diffraction analyses were carried out by using Philips Analytical X-Ray BV, diffractometer type PW 1840. Radiation was provided by copper target (Cu anode 2000 W) high intensity X-ray tube operated at 40 KV and 25 mA. Divergence and the receiving slits were 1 and 0.2, respectively. The antibacterial and antifungal activities were evaluated at the Microbiological laboratory, Microanalytical center, Cairo University, Egypt. The anticancer activity was performed at the National Cancer Institute, Cancer Biology Department, Pharmacology Department, and Cairo University. The optical density (O.D.) of each well was measured spectrophotometrically at 564 nm with an ELIZA microplate reader (Meter tech. S 960, U.S.A.).

General procedure for synthesis

An ethanolic solution 15ml of lomefloxacin (LFX) with 0.351 g (1 mmol) was added to an aqueous solution of the metal salts. This is followed by the addition of an ethanolic solution 12 ml of dl-alanine (Ala) with 0.092 g (1 mmol). After constant stirring (1 hour) using appropriate amounts of materials needed as decided by the molar ratio 1:1:1 (M:LFX:Ala). Successively, the resulting precipitates were filtered off, washed several times and recrystallized with 1:3 (v/v) ethanol : water mixture. Then, it was dried in an oven at 65°C

Biological activity

A filter paper disk (5mm) was transferred into 250 mL flasks containing 20 mL of working volume of tested solution (100 g/mL). All flasks were autoclaved for 20 min at 121°C. LB agar media surfaces were inoculated with two investigated bacteria (gram positive and gram negative) and two strains of fungi then, transferred to a saturated disk with a tested solution in the center of Petri dish (agar plates). Finally, all these Petri dishes were incubated at 25 °C for 48 h where clear or inhibition zones were detected around each disk. Control flask of the experiment was designed to perform under the same condition described previously for each microorganism but with dimethylformamide solution only and by subtracting the diameter of inhibition zone resulting with dimethylformamide from that obtained in each case, so antibacterial activity could be calculated [27]. All experiments were performed as triplicate and data plotted were the mean value.

Anticancer activity

Potential cytotoxicity of the compounds was tested using the method of Skehan et al 28. Cells were plated in 96-multiwell plate (104cells/well) for 24 h before treatment with the compounds to allow attachment of cell to the wall of the plate. Different concentrations of the compounds under investigation (0, 5, 12.5, 25, 50 and 100 µg/ml) were added to the cell monolayer triplicate wells were prepared for each individual dose. The monolayer cells were incubated with the compounds for 48 h at 37 °C and in 5% CO_2 atmosphere. After 48 h, cells were fixed, washed and stained with SRB stain. Excess stain was washed with acetic acid and attached stain was recovered with tris-EDTA buffer. The optical density (O.D.) of each well was measured spectrophotometrically at 564 nm with an ELIZA microplate reader and the mean background absorbance was automatically subtracted and mean values of each drug concentration was calculated. The relation between surviving fraction and drug concentration is plotted to get the survival curve of Breath tumor cell line for each compound.

Calculation

The percentage of cell survival was calculated as follows:

Survival fraction = O.D. (treated cells)/ O.D. (control cells).

The IC_{50} values are the concentrations of thymoquinone required to produce 50 % inhibition of cell growth. The experiment was repeated 3 times for each cell line.

RESULTS AND DISCUSSIONS

The prepared complexes were found to be coloured, insoluble in most common organic solvents such as chloroform, acetone and acetonitrile but completely soluble in dimethylsulfoxide and dimethylformamide. The high values observed of molar conductivities in DMF indicate the electrolyte behavior of the complexes. Elemental analysis (C, H, N) and metal determination were in good agreement with general formula given for the complexes. Table 1 gives the physical properties of the complexes.

Magnetic susceptibility

The observed magnetic moment values for the prepared complexes (Table 1), indicates that Zn(II), Th(IV) and UO_2(II) complexes are diamagnetic and according to their molecular formula an octahedral arrangement of the ligand molecules around the central metal ion is proposed. However, Cr(III), Mn(II), Fe(III), Co(II), Ni(II) and Cu(II) complexes showed normal measured value of µeff for octahedral structure (Table 1) [29-31].

Electronic spectral studies

The absorption spectra of LFX ternary chelates with alanine, at wavelength ranging from 200 to 600 nm are carried out in ethanol. The band at 320 nm may be assigned to $n \rightarrow \pi^*$ transition within the C=O group or carboxylate

Table (1). Analytical and physical data of LFX and its ternary complexes with Alanine.

Compound (Chemical formula)	Color (%Yield)	M.p.(°C)	% Found (Calcd)				$\mu_{eff.}$ (B.M.)	A_m
			C	H	N	M		$W^{-1}mol^{-1}cm^2$
[Cr(LFX)(Ala)]·Cl_2 ($C_{20}H_{25}Cl_2CrF_2N_4O_3$)	Dark green(91)	280	32.75(35.57)	4.88(4.46)	9.72(9.60)	8.99(9.23)	3.42	149
[Mn(LFX)(Ala)]·Cl($C_{20}H_{25}ClF_2N_4O_3Mn$)	Pale brown(93)	250	37.99(37.82)	4.80(4.72)	10.75(10.59)	10.02(10.21)	5.36	112
[Fe(LFX)(Ala)(H_2O)$_2$]Cl_2·H_2O($C_{20}H_{31}Cl_2F_2FeN_4O_6$)	Brown(85)	240	41.04(40.81)	5.54(5.27)	9.71(9.52)	9.32(9.52)	5.61	156
[Co(LFX)(Ala)(H_2O)$_2$]·Cl ($C_{20}H_{29}ClCoF_2N_4O_5$)	Dark blue(72)	210	42.54(42.12)	5.12(5.09)	10.02(9.82)	10.64(10.35)	5.40	110
[Ni(LFX)(Ala)(H_2O)$_2$]Cl·H_2O ($C_{20}H_{31}ClF_2N_4NiO_6$)	Green(87)	260	43.79(43.20)	5.98(5.95)	10.14(10.08)	10.26(10.62)	3.21	126
[Cu(LFX)(Ala)(H_2O)$_2$]Cl·2H_2O ($C_{20}H_{33}ClCuF_2N_4O_7$)	Dark Blue(86)	220	41.72(41.52)	5.95(5.71)	9.81(9.67)	10.71(10.96)	1.95	120
[Zn(LFX)(Ala)(H_2O)$_2$]·Cl ($C_{20}H_{29}ClF_2N_4O_5Zn$)	White(73)	230	41.93(41.66)	5.25(5.03)	9.74(9.72)	11.10(11.34)	Diam.	130
[Th(LFX)(Ala)]·Cl_3 ($C_{20}H_{25}Cl_3F_2N_4O_3Th$)	Pale yellow(74)	220	30.96(30.86)	3.23(3.21)	7.61(7.20)	29.65(29.83)	Diam.	318
[UO_2(LFX)(Ala)]·(NO_3)] ($C_{20}H_{25}F_2N_5O_{10}U$)	Yellow(79)	200	28.89(28.81)	3.01(2.96)	8.43(8.17)	35.45(35.86)	Diam.	135

Table (2). IR spectra (4000-400 cm^{-1}) of LFX (L), alanine (A) and their ternary metal complexes.

LFX	Alanine (Ala)	[Cr(LFX)(Ala)(H_2O)$_2$]Cl_2.$2H_2O$	[Mn(LFX)(Ala)(H_2O)$_2$]Cl.$2H_2O$	[Fe(LFX)(Ala)(H_2O)$_2$]Cl_2.$2H_2O$	[Co(LFX)(Ala)(H_2O)$_2$]Cl.$2H_2O$	[Ni(LFX)(Ala)(H_2O)$_2$]Cl.H_2O	[Cu(LFX)(Ala)(H_2O)$_2$]Cl.$2H_2O$	[Zn(LFX)(Ala)(H_2O)$_2$]Cl.$2H_2O$	[Th(LFX)(Ala)(H_2O)$_2$]Cl_3.$2H_2O$	[UO_2(LFX)(Ala)](NO_3)	Assignment
3367br	-	3389br	3293br	3376br	3376br	3415br	3389br	3441br	3376br	3441br	OH stretching
-	3084br	3050br	3050br	3102br	3140br	3051br	3054br	3053br	3034br	3100br	Asym. NH_3 stretch
-	2934s	2934s	2883s	2974s	2896s	2908s	2963s	2830s	2927s	2941s	CH stretch in CH_3
-	2602m	2632s	2612s	2618s	2633s	2574s	2603s	2618s	2617s	2632s	NH stretch in NH_3
1725sh	1703s	1724m	dis	dis	dis	dis	1724sh	1712m	dis	1765s	C=O stretch
1590s	1574m	1559s	1567m	1551s	1574s	1574m	1588s	1559s	1581s	1588s	COO asym.
-	1519m	1523sh	1522s	1523sh	1522s	1529s	1524s	1515s	1530s	1523m	NH_2 scissoring
-	1455sh	1453m	1456s	1455m	1470s	1471m	1469m	1456s	1456s	1463s	CH_3 deformation
1396s	1413sh	1412s	1412s	1406m	1398s	1397m	1368s	1412s	1406s	1419s	COO sym.
-	1362sh	1382sh	1383s	1355s	1323s	1338sh	1338s	1368s	1323s	1384m	CH_3 puckering
808sh	849sh	838sh	889sh	850sh	838s	838s	851m	849sh	849sh	857m	C-N stretch+ C_2-C_4 stretch
-	649sh	647s	651sh	662s	658sh	659sh	662s	665sh	657sh	658sh	OCOH+ NH_2 bend
-	540sh	541s	540m	541sh	544s	544s	560m	541sh	540sh	540m	OH bend
-	-	518s	502sh	502s	497s	502s	502s	493s	502s	502m	M-O
-	-	485s	456sh	449s	456s	456s	449s	456s	456s	471s	M-O in coordinated water
-	-	412s	411s	419s	427s	427s	419s	427s	412s	411s	M-N

sh = sharp, m = medium, br = broad, s = small, w = weak

group of free ligand. This band is red shifted to 321-326 nm in some chelates, while it disappeared in all the remaining chelates revealing the involvement of the C=O group of LFX ligand and carboxylate–O of amino acids in chelate formation[32, 33].

The n → π* transition within the LFX molecule is overlapped with those of alanine molecule at λ = 320–350 nm so renders it difficult to attribute the blue or red shift of these bands as a result of the involvement of the N atom of LFX or amino group of alanine during chelate formation (N→ M) [32, 33].

The diffused reflectance spectrum of Co(II) complex shows bands at 13,122, 15,239 and 22,041 cm^{-1} which are attributed to the electronic transition $^4T_{1g}(F) \rightarrow {}^4T_{2g}(F)$ (ν_1), $^4T_{1g}(F) \rightarrow {}^4A_{2g}(F)$ (ν_2) and $^4T_{1g}(F) \rightarrow {}^4T_{1g}(P)$ (ν_3), respectively, suggesting that there is an octahedral geometry around Co(II) ion [31,32]. The region at 28,285 cm^{-1} refers to the charge transfer band. The exhibited diffused absorption bands of Ni(II) complex at 13,256, 14,780 and 20,888 cm^{-1} are attributed to the electronic transition $^3A_{2g}(F) \rightarrow {}^3T_{1g}(P)$, $^3A_{2g}(F) \rightarrow {}^3T_{1g}(F)$ and $^3A_{2g}(F) \rightarrow {}^3T_{2g}(F)$. The spectrum shows also band at 26,615 cm^{-1} which may be attributed to ligand to metal charge transfer [29].

The diffused spectrum of Cu(II) complex shows that its bands in the visible region is attributed to the electronic transitions of $^2A_{1g}(D) \rightarrow {}^2B_{1g}(D)$ and $^2E_g(D) \rightarrow {}^2B_{1g}(D)$ at 15,096 and 21,529 cm^{-1}, respectively which confirm the octahedral geometry. The diffused reflectance spectrum of Cr(III) complex exhibits bands at 13,598; 25,574 and 28,048 cm^{-1}, respectively, which assigned to $^4A_{2g}(F) \rightarrow {}^4T_{2g}(F)$, $^4A_{2g}(F) \rightarrow {}^4T_{2g}(F)$ and $^4A_{2g}(F) \rightarrow {}^4T_{2g}(P)$ spin allowed *d-d* transitions. These bands suggest an octahedral geometry for the Cr(III) complexes [29, 34].

The diffused reflectance spectrum of the Mn(II) complex shows three bands at 16,542;19,850 and 25,880 cm^{-1} assignable to $^4T_{1g} \rightarrow {}^6A_{1g}$, $^4T_{2g}(G) \rightarrow {}^6A_{1g}$ and $^4T_{1g}(D) \rightarrow {}^6A_{1g}$ transitions, respectively [29], which indicate that the complexes have octahedral geometry. From the diffused reflectance spectrum, it is observed that, the Fe(III) complex exhibits bands at 12,578, 16,039 and 21,522 cm^{-1}, which may be assigned to the $^6A_{1g} \rightarrow {}^5T_{2g}(G)$ and $^6A_{1g} \rightarrow {}^5T_{1g}$ transitions in octahedral geometry of the complex 35. The spectrum shows also a band at 24,591 cm^{-1} which may be attributed to ligand to metal charge transfer.

Infrared spectral studies

(1)The υ(C=O) stretching vibration is found at 1725 cm^{-1} in the LFX free ligand as sharp intense band[30-33]. This band is found in the spectra of the ternary complexes at 1722-1739 cm^{-1} (Table 2) or disappeared in some complexes[36]. The shift of the carbonyl group band to higher or lower wavenumbers or its disappearance in the complexes can be attributed to the participation of the carbonyl oxygen atoms of LFX ligand in coordination to the metal ions (M—O) .

(2)The υ(OH), υ_{asym}(COO) and υ_{sym}(COO) stretching vibrations are observed at 3367, 1590 and 1396 cm^{-1}, respectively, for LFX free ligand [30-33]. The OH stretching vibration; υ(OH), is found to shift to lower wavenumbers in the range 3037-3263 cm^{-1} in the spectra of the ternary complexes. The participation of the carboxylate O atom of LFX drug in the complexes formation is evidenced from the shift in position of these bands to 1530-1574 and 1396-1413 cm^{-1}, respectively, for ternary complexes (Table 2). The bands at the wavenumber 1703, 1588 and 1474 cm^{-1} regions, in the free amino acid; Ala, are assigned to the carbonyl, antisymmetric and symmetric stretching vibrations of the carboxylate group, respectively [30-

[33]. The shift of these bands to higher or lower frequencies suggests the participation of –COOH group in complex formation after deprotonation [36]. The values of band shift $\Delta\upsilon$ (υ_{asym}(COO) – υ_{sym}(COO)) are all about 143–205 cm^{-1}, indicating that the carboxylate group in Ala are chelated in a uni-negatively manner to the metal ions [36].

(3)At the wavenumber 3500–3000 cm^{-1} region of the ternary chelates, the overlap of the various υ(NH) vibrations coupled in many cases with molecules of water of hydration gives rise to very strong absorption. This prevents the individual recognition of the various bands. The asymmetric NH_2 stretching, NH_2 scissoring and NH_2 bending are found in the spectra of the free alanine ligand at 3084, 1519 and 649 cm^{-1}, respectively [29-31]. The participation of the NH_2 group in chelation is evidenced from the shift of the band to lower or higher wavenumbers to the extent of 12–30 cm^{-1} in all the complexes confirming coordination of the NH_2 group to the metal ions [31-33](Table 2).

(4)New bands are found in the spectra of the ternary complexes in the region 493-574 which are assigned to υ(M-O) stretching vibrations of carbonyl oxygen, carboxylate oxygen and coordinated water. The metal–oxygen stretching frequencies could not be assigned unambiguously due to the presence of three types of υ(M-O) vibrations i.e., M–COO–, M–H_2O and M–C=O. The bands at 411-456 cm^{-1} have been assigned to υ(M-N) stretching vibration. This is ensured the participation of amino group in the complex formation.

Most of the band shifts observed at the wavenumber region 1150–994 cm[are in agreement with the structural changes observed in the molecular carbon skeleton after complexation, which cause some important changes in (C–C) bond lengths and also affect some of the C–O and C–N bonds indirectly [30-33]. These bands can be as:

(I) The (C-C and C-N) stretching vibrations are found at 808, and 849 cm-1 for LFX, and alanine free ligands spectra, respectively 29-31. These bands are shifted to higher or lower wavenumbers at 838-889 and 1033-1052 cm-1 (Table 2).

(II) The CH_3 puckering, CH_3 deformation and CH stretching in CH_3 bands are observed at 1362, 1455 and 2943 cm^{-1}, respectively, for alanine free ligand [29-31, 36]. These bands are shifted in position to 1383-1323, 1453-1471 and 2927-2974 cm^{-1}, respectively, for M-LFX-Ala complexes (Table 2).

Therefore, from the IR spectral studies, it is concluded that:

(a) LFX behaves as a neutral bidentate ligand with OO coordination sites and coordinated to the metal ions via the carbonyl oxygen and protonated carboxylic oxygen.

(b) dl-alanine behaves as a uninegatively bidentate ligand where it binds to the central metal ions through its deprotonated carboxylate group and its amino group.

^{1}HNMR spectra

A survey of literature revealed that the NMR spectroscopy has been proved useful in establishing the nature and structure of fluoroquinolone antimicrobials as well as their complexes in solutions[37]. The 1H NMR spectrum of lomefloxacin was recorded in d6-dimethylsulfoxide (DMSO-d6) solution using tetramethylsilane (TMS) as internal standard.

The ^{1}H-NMR spectral data for [[Zn(LFX)(Ala)$(H_2O)_2$]•Cl and its deuterated spectrum were found that:

•The aryl protons in LFX, 2-H and 5-H, were easily distinguished since 5-H showed splitting due to the coupling with the 19F nucleus at the adjacent position. Thus, the doublets at 7.89 ppm was assigned to the 5-H of LFX. 38 This signal is found to be shifted to 7.87, 7.85 and 7.87 ppm for Zn-LFX-Ala complex.

•The bands observed at 8.93, 8.91, 8.87 and 8.88 ppm (s, H, CH of carbon 2) and 3.39, 3.27, 3.02 and 3.29 ppm (d, H, CH of carbon 3') are assigned to the CH proton 30, 31.

•The bands observed at 3.39, 3.40, 3.41 and 3.44 ppm (d, 4H, CH_2 of carbon 5', 6') and 3.55, 3.37, 3.37 and 3.40 ppm (d, 2H, CH_2 of carbon 2') are assigned to the CH2 protons.

•The bands observed at 1.46, 1.48, 1.46 and 1.47 ppm are assigned to (d, 3H, CH_3 of carbon 1b) in addition to the bands observed at 1.44, 1.44, 1.44 and 1.45 ppm (d, 3H, CH_3 of carbon 3a'). These bands are assigned to the CH proton 30, 31.

•Upon comparison with the free LFX ligand, the signal observed at 13.5 ppm can be assigned to the carboxylate OH. This signal disappears in the spectra of the complexes in accordance with the IR spectral data. Although the LFX ligand coordinated to the metal ions without proton displacement, the disappearance of this signal can be attributed to Zwitter-ion formation shown in scheme (5)[36, 4].•

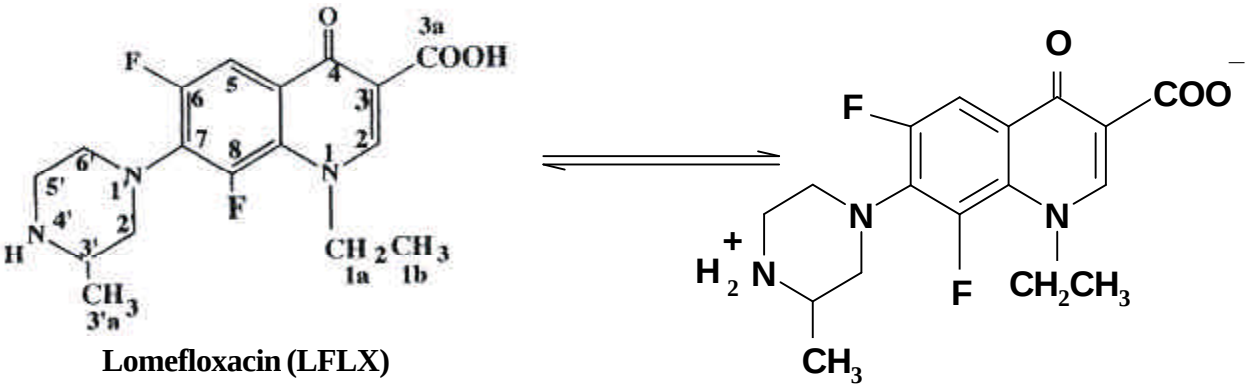

Scheme (1). Zwitter-ion formation of LFX.

Due to the different chemical environments, a signal is recorded for the nitrogen (NH) of free LFX ligand at 2.50 ppm.

Therefore, it is clear from these results that the data obtained from the elemental analyses; IR and 1H NMR spectral measurements are in agreement with each other.

X-ray powder diffraction

X-ray powder diffraction pattern in the 0θ< 2θ < 60θ of the LFX, and alanine ligands and the metal complexes were carried out in order to give an insight about the lattice dynamics of these compounds. The X-ray powder diffraction obtained reflects a shadow on the fact that each solid represents a definite compound of a definite structure which is not contaminated with starting materials.

XRD analysis for ternary chelates shows that the coordination of LFX alone or in the presence of Ala to the metal ions changes the XRD pattern of the ligands. This means that the metal ions are not fitted in the same phase of LFX or Ala. Therefore, the non-similarity of XRD pattern between the metal ions and ternary chelates suggests that these chelates have a different phase structures than the LFX, and Ala ligands. In addition, on comparing the XRD spectra of the ternary chelates with the XRD spectra of the free ligands, indicate the crystallinity of the ternary chelates under study, except [Co(LFX)(Ala)$(H_2O)_2$]•Cl and [UO_2(LFX)(Ala)]•(NO_3)] chelates, where they can considered as amorphous structures.

Thermal analyses (TG, DTG and DTA) of the metal chelates

The thermogram of [Fe(LFX)(Ala)$(H_2O)_2$]Cl_2•H_2O chelate shows five decomposition steps within the temperature range 50-650 °C as illustrated in Table (3). The first step of decomposition within the temperature range 30-90°C, shows loss of water molecule of hydration with a mass loss 2.62% (calcd. 2.90%). The second stage at temperature range 130-230°C corresponds to the loss of two molecules of coordinated water and the loss of Cl_2 gas with weight loss 18.31% (calcd. 17.28%). The subsequent steps in the ternary chelates within the temperature ranges given in Table (3) corresponds to the removal of the organic part of the ligands leaving metal oxide as a residue. The overall weight loss amounts to 87.63% (calcd. 86.76%). The DTA data listed in Table (3) showed that these mass losses are accompanied by exothermic (288, 325, 456 and 581°C) and endothermic (221°C) peaks.

On the other hand [Ni(LFX)(Ala)$(H_2O)_2$]Cl•H_2O chelate exhibits three decomposition steps. The first step corresponds to the loss of the water molecules of hydration in the temperature rang 30-100°C (mass loss = 2.34% (calcd. 3.06%)). The second stage within the temperature range 100-285°C corresponds to the loss of two molecules of coordinated water with weight loss 5.95% (calcd. 6.11%). In the third step, the mass loss within the temperature range 250-800°C corresponds to the removal of the organic part of the ligands leaving metal oxide as a residue. The DTA data are listed in Table (3). It is clear from these data that these mass losses are accompanied by exothermic (335, 490 and 621°C) peaks.

The TG curve of , [Cu(LFX)(Ala)$(H_2O)_2$]Cl•$2H_2O$ chelate shows four decomposition steps within the temperature range 30-700°C as illustrated in Table (3). The first step for the Cu(II) complex is the loss of the water of hydration in the temperature range 35-120°C (mass loss = 4.62% (calcd. 5.90%)). The second stage within the temperature range 120-225°C corresponds to the loss of coordinated water molecules and the loss of HCl gas and removal of apart of organic ligand with weight loss 16.62 % (calcd. 15.25%). The subsequent steps (225-700 °C) correspond to the removal of

Table (3). Thermoanalytical results (TG, DTG and DTA) of LFX and its metal ternary complexes with alanine.

Complex	TG range (°C)	DTG_{max} (°C)	n*	Mass loss Total mass loss Estim (Calcd) %	Assignment	Metallic residue	DTA (°C)
Alanine	170-330	264	1	99.09 (100.0)	-Loss of $C_3H_7NO_2$	-	272(+)
[Fe(LFX)(ala)$(H_2O)_2$]Cl_2·H_2O	30-90	59	1	2.62 (2.90)	- Loss of H_2O.		221(+), 288(-), 325(-),
	130-230	214.57	1	18.31 (17.28)	- Loss of $2H_2O$ and Cl_2.	½ Fe_2O_3	456(-), 581(-)
	230-630	290, 399, 580	3	66.73 (66.60) 87.63 (86.76)	- Loss of $C_{20}H_{25}F_2N_4O_{3.5}$.		
[Ni(LFX)(Ala)$(H_2O)_2$]Cl·H_2O	30-100	56	1	2.34 (3.06)	- Loss of H_2O.		335(-), 490(-), 621(-)
	100-285	262	1	5.95 (6.11)	- Loss of $2H_2O$.	NiO	
	285-780	353	1	78.94 (78.07) 87.23 (87.25)	- Loss of $C_{20}H_{26}Cl\ F_2N_4O_4$.		
[Cu(LFX)(Ala)$(H_2O)_2$]Cl·$2H_2O$	35-120	68	1	4.62 (5.90)	- Loss of $2H_2O$.		69(-), 219(+), 281(+),
	120-225	202	1	16.62 (15.25)	- Loss of $2H_2O$, HCl and CH_3NO.	CuO	455(-), 577(-)
	225-630	364, 579	2	61.22 (61.77) 82.07 (82.92)	- Loss of $C_{19}H_{21}F_2N_3O_3$.		
[UO_2(LFX)(Ala)]·(NO_3)	80-370	224	1	34.078 (34.37)	- Loss of NO_3 and $C_{12}H_{12}F_2N_2O_4$.	UO_2	232(-), 517(-)
	370-710	520	1	18.58 (18.51) 52.66 (52.08)	- Loss of $C_8H_{14}N_2O$.		

Table (4). Thermodynamic data of the thermal decomposition of ternary complexes of LFX and alanine.

Complex	Decomp. Temp. °C	E* kJmol^{-1}	A s^{-1}	ΔS* KJmol^{-1}	ΔH* kJmol^{-1}	ΔG* kJmol^{-1}
Alanine	170-330	20.54 x10^4	7.46x10^{23}	213.1	20.32	43.65
[Fe(LFX)(ala)$(H_2O)_2$]Cl_2·H_2O	30-90	30.77	1.25×10^6	-120.7	29.77	44.37
	130-230	85.07	2.49×10^5	-145.9	80.91	153.9
	230-630	41.11	7.59×10^5	-138.8	35.68	126.3
[Ni(LFX)(Ala)$(H_2O)_2$]Cl·H_2O	30-100	31.73	4.71×10^5	-126.8	30.94	43.03
	100-285	79.35	4.69×10^6	-116.3	77.10	108.5
	285-780	219.8	5.15×10^1	-7.24	214.8	219.1
[Cu(LFX)(Ala)$(H_2O)_2$]Cl·$2H_2O$	35-120	38.21	5.92×10^6	-120.7	37.73	44.68
	120-225	32.78	9.82×10^6	-109.3	30.77	57.10
	225-630	102.9	3.83×10^7	-100.9	100.1	135.0
[UO_2(LFX)(Ala)] ·(NO_3)	80-370	55.40	3.48×10^5	-139.1	52.82	95.95
	370-710	158.1	3.44×10^5	-46.83	154.3	175.8

the organic part of the ligands leaving metal oxide as a residue. The overall weight loss amounts is 82.07% (calcd. 82.92%). The DTA data are listed in Table (3). It is clear from these data that these mass losses are accompanied by exothermic (69, 455 and 577°C), and endothermic (219 and 281°C) peaks.

The TG curve of the UO_2(II) chelate indicates that the complex is decomposed in two stage as illustrated in Table (3). The first step of decomposition within the temperature range 80-370 °C correspond to the loss of nitrate molecules and apart of organic ligand with a mass loss of 34.08% (calcd. 34.37%). The remaining step (370-710 °C) corresponds to the removal of the organic part of the ligands leaving metal oxide as a residue. The overall weight loss amounts to 82.07% (calcd. 82.92%) .

The DTA data clearfy that the mass losses are accompanied by exothermic peaks at 69, 455 and 577°C and endothermic peaks at 219 and 281°C Table(3).

Kinetic studies

In order to assess the effect of the metal ion on the thermal behavior of the complexes, the order n, and the heat of activation E of the various decomposition stages were determined from the TG and DTG. Several techniques have been used for the evaluation of temperature integral. Most commonly used methods for this purpose are the differential method of Freeman and Carroll 39 integral methods of Coat and Redfern 40, the approximation method of Horowitz and Metzger 41. The kinetic parameters for the ternary complexes are evaluated using the Coats-Redfern method and the results are summarized in Table 4.

The entropy of activation, ΔS*, the enthalpy of activation ΔH*, and Gibbs free energy, ΔG*, were calculated. The data tabulated reveals that the activation energy E increases somewhat through the degradation steps revealing the high stability of the remaining part suggesting a high stability of complexes. The negative ΔS* values indicate the activated fragment has ordered structures. In addition, the positive ΔH* reflects the endothermic decomposition process, while the positive ΔG* sign reveals that the free energy of the final residue is higher than that of the initial compound, and the decomposition stages are non-spontaneous. This results from increasing TΔS* clearly from one step to another which override the values of ΔH* reflecting that the rate of removal of the subsequent species will be lower than that of the precedent one[42].

Structural interpretation

The structures of the ternary complexes of LFX with Cr(III), Mn(II), Fe(III), Co(II), Ni(II), Cu(II), Zn(II), UO_2(II) and Th(IV) ions are confirmed by the elemental analyses, IR, ^{1}H NMR, molar conductance, magnetic moment, solid reflectance, UV-vis, XRD and thermal analyses (TG and DTA) data.

Therefore, from the IR spectral studies, it is concluded that:

(a)LFX behaves as a neutral bidentate ligand with OO coordination sites and coordinated to the metal ions via the carbonyl oxygen and protonated carboxylic oxygen.

(b) dl-alanine behaves as a uninegative bidentate ligand with NO donor sites and coordinated to the metal ions via the amino group N and deprotonated carboxylic oxygen.

From the molar conductance data (Λm), it is concluded that the complexes of the Fe(III) and Cr(III) are considered as 1:2 electrolytes. In addition, the results indicate also that M(II) complex is considered of the type 1:1 electrolyte. Meanwhile, Th(VI) complex is considered as 1:3 electrolyte.

The ^{1}H NMR spectra of the free ligands and the diamagnetic Zn(II) complex shows that the protonated COOH signal of LFX ligand participate in chelation. While in case of ternary complexes, the spectra show that the protonated COOH signal of LFX ligand and NH_2 and deprotonated COOH signal of alanine amino acid involved in chelation with metal ions. The OH signal disappears in the spectra of the complexes in accordance with the IR spectral data. Although the LFX ligand coordinated to the metal ions without proton displacement, the disappearance of this signal can be attributed to Zwitter-ion formation[43-51].

XRD data suggest that the LFX ligand and its ternary chelates under study are crystalline, except [Co(LFX)(Ala)$(H_2O)_2$]•Cl and [UO_2(LFX)(Ala)]•(NO_3)] chelates, it can considered as amorphous structure. On the basis of the above observations and from the magnetic and solid reflectance measurements, octahedral geometry is suggested for the investigated complexes. The structures of complexes are shown in Figure (1).

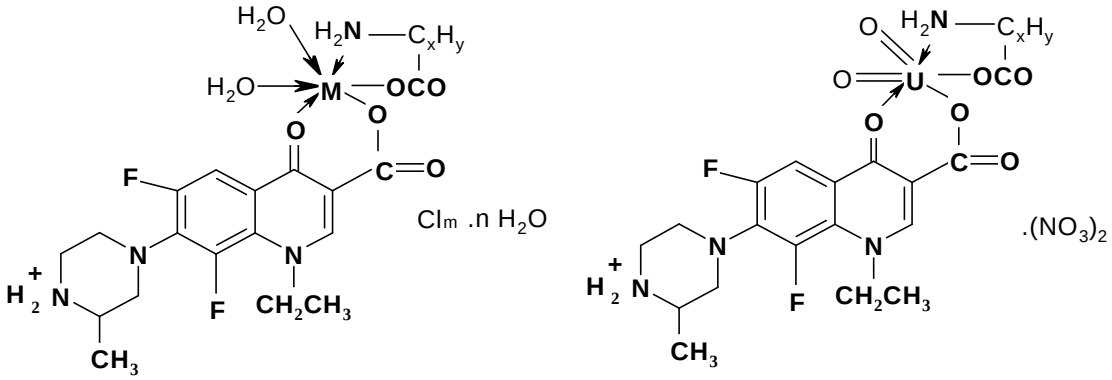

M = Cr(III), Mn(II), Fe(III),Co(II), Ni(II), Cu(II), Zn(II) and Th(IV) .
m = 1-3, n = 0-2, C_xH_y = -CHCH$_3$

Figure (1). Structural formulae of LFX and its ternary complexes.

Biological activity

Antimicrobial activity

On comparing the biological activity of the LFX and its ternary complexes, in general, the synthesized metal complexes have higher biological activities compared to the free ligands. The increased inhibition activity of the metal complexes can be explained on the basis of Tweedy's chelation theory 52. In metal complexes, on chelation the polarity of the metal ion will be reduced to a greater extent due to the overlap of the ligand orbital and partial sharing of the positive charge of the metal ion with donor groups. Further, it increases the delocalization of p- electrons over the whole chelate ring. Chelation not only reduces the polarity of metal ion, but also increases the lipophilic character of the chelate and makes it easy to permeate through the cell membrane of the bacterium 39 and enhances the penetration of the metal complexes into lipid membranes and blocks the metal binding sites in the enzymes 53. Studies for the interaction between metal cations and fluoroquinolones antibacterial in the literature 54–55 have shown that the proposed mechanism was based on the chelation between metal and the carbonyl and carboxyl groups. In general, the synthesized metal complexes have higher biological activities compared to the free ligands. Metal complexes also disturb the respiration process of the cell and thus block the synthesis of proteins, which restricts further growth of the organisms. The results are as follows.

Bacteria

It is obvious from the result (Table (5) and Fig. 2) that the biological activity against the two gram positive and gram negative bacteria of all ternary metal complexes is higher than that of the LFX drug, alanine ligands and tetracycline standard images.

(a) Gram-negative bacteria

The biological activity has the order UO_2(II) > Zn(II) > Co(II) > Fe(III) >LFX = Th(IV) > Mn(II) > Ni(II) = Cu(II) = Cr(III) > tetracycline > alanine for *E. coli* and Cr(III) > LFX = Mn(II) = Cu(II) > Co(II) = Ni(II) > Fe(III) = Zn(II) >Th(IV) = UO_2(II) > tetracycline > alanine for *Neisseria gonorrhoeae* bacteria.

(b) Gram-positive bacteria

The biological activity has the order Co(II) = Cr(III) > Ni(II) > Cu(II) > Mn(II) > Zn(II) > Th(IV) = UO_2(II) = Fe(III) > tetracycline > LFX = alanine = 0 for *Staphylococcus aureus* and has the order Cr(III) > Mn(II) = Cu(II) > Co(II) = Ni(II) > Fe(III) = Zn(II) > Th(IV) = UO_2(II) > tetracycline > LFX > alanine for *Bacillus subtilis*.

(a) Using *Aspergillus flavus* fungus

The results showed that there is no antifungal activity for the free LFX ligand or its complexes toward this organism.

(b) Using *Candida albicans* fungus

The biological activities of the ternary complexes are found to be higher than that of the free LFX ligand but lower than amphotricine standard except Co(II) and Ni(II) complexes. The biological activity is found to follow the order:

Ni(II) > Co(II) > amphotricine standard > Fe(III) > Cu(II) = Cr(III) = Zn(II) = UO_2 (II) = Th(IV) > Mn(II) = LFX.

The importance of this lies in the fact that these complexes could be applied fairly in the treatment of some common diseases caused by *E. coli* e.g. Septicaemia, Gastroenteritis, Urinary tract infections and hospital acquired infections 56. However, the complexes were specialized in inhibiting Gram-positive and Gram-negative bacterial strains. The importance of this unique property of the investigated complexes lies in the fact that, it could be applied safely in the treatment of infections caused by any of these particular strains.

Table (5). Biological activity of ternary M-LFX-ala complexes.

Sample	Inhibition zone diameter (mm / mg sample)			
	E. coli	*Neisseria gonorrhoeae*	*Staphylococcus aureus*	*Bacillus subtilis*
Control: DMSO	0.0	0.0	0.0	0.0
LFX	43	44	0.0	11
Alanine	10	9	0.0	10
[Cr(LFX)(Ala)]·Cl2	40	45	45	45
[Mn(LFX)(Ala)]·Cl	42	44	40	44
[Fe(LFX)(Ala)(H_2O)$_2$]Cl_2·H_2O	44	40	35	40
[Co(LFX)(Ala)(H_2O)$_2$]·Cl	45	42	45	42
[Ni(LFX)(Ala)(H_2O)$_2$]Cl·H_2O	40	42	43	42
[Cu(LFX)(Ala)(H_2O)$_2$]Cl·2H_2O	40	44	42	44
[Zn(LFX)(Ala)(H_2O)$_2$]·Cl	46	40	37	40
[Th(LFX)(Ala)]·Cl_3	43	38	35	38
[UO_2(LFX)(Ala)].(NO_3)]·3H_2O	49	38	35	38
Standard Tetracycline	34	33	30	30

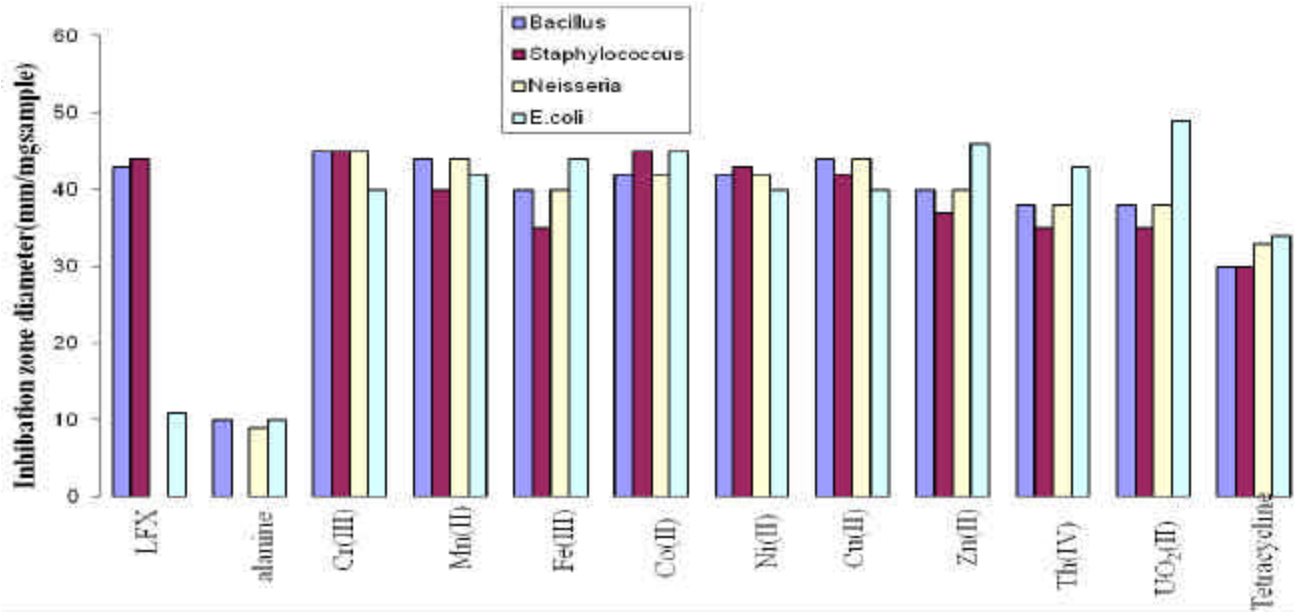

Figure (2). Biological activity of LFX and its ternary complexes with alanine.

Cytotoxic activity

The LFX drug, alanine and the ternary metal complexes were tested for their activity against breast cancer cell line (MCF7) by using 100 µg / ml drug concentration. From these result (Table (6) and Fig.(3)), it is clear that LFX and its metal complexes of Mn(II), Co(II), Ni(II), Cu(II) and Zn(II) metals were found to be very active against breast cancer cells with inhibition ratio values between 70-85.5 %, while other complexes utilized in this work had been shown to be inactive (less than 70% inhibition). It is clear that a pattern of activity can be determined using different drug concentrations (Table 6) and Fig. (3)). The IC_{50} values are found to be 11.2-46 and follow the order $[Ni(LFX)(Ala)(H_2O)_2]Cl{\bullet}H_2O$ =LFX > $[Zn(LFX)(Ala)(H_2O)_2]{\bullet}Cl$ > $[Co(LFX)(Ala)(H_2O)_2]{\bullet}Cl$ > [Mn(LFX)(Ala)]•Cl .While alanine and other complexes had been shown to be inactive at lower concentration than 100 µg / ml. The results may be due to the presence of chloride ion in complexes which may enhanced antimicrobial activity due to the formation of hypochlorous acid that formed when free chloride upon oxidation resulting into chlorine that reacts with water to yield hypochlorous acid[57]. The formed acid was, further decomposes to hydrochloric acid and oxygen. The later, a strong oxidizing agent destroys microbes by oxidizing cellular components [42]. Antimicrobial action of chlorine compounds is also may be due to the combination of chlorine with proteins and enzymes of membranes.

Table (6). Antibreastic cancer activity of LFX and its alanine ternary complexes

Complex	Surviving fraction (MCF7)					IC_{50}
Concn.(µg/ ml)	0.0	5	12.5	25	50	(µg/ ml)
LFX	1.00	0.64	0.53	0.27	0.19	14.0
[Mn(LFX)(Ala)]·Cl	1.00	0.76	0.69	0.57	0.49	46.0
$[Co(LFX)(Ala)(H_2O)_2]{\cdot}Cl$	1.00	0.72	0.57	0.26	0.18	15.6
$[Ni(LFX)(Ala)(H_2O)_2]Cl{\cdot}H_2O$	1.00	0.54	0.54	0.21	0.21	14.0
$[Cu(LFX)(Ala)(H_2O)_2]Cl{\cdot}2H_2O$	1.00	0.96	0.86	0.63	0.71	-
$[Zn(LFX)(Ala)(H_2O)_2]{\cdot}Cl$	1.00	0.83	0.56	0.26	0.21	14.9

Figure (3). Anticancer activity of LFX and its ternary complexes with alanine.

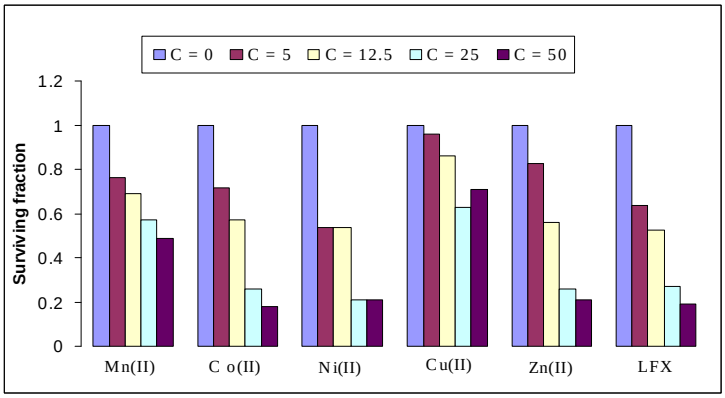

using the different spectral and physicochemical studies. The analytical and spectral data reveal that the synthesized complexes exhibit octahedral geometry around the central metal ions. The results of in-vitro biocidal activities of the ligand and its metal complexes clearly show that the compounds have both antibacterial and antifungal potency against the tested organisms. The complexes showed more activity than free ligand. Further investigations on their antitumor activity revealed that such complexes possessed a considerable antitumor activity which was thought to be related with its DNA-binding affinity.

REFERENCES

[1] Mitscher,-LA. Chem. Rev. 105: 559-592 (2005).
[2] Andriole,-VT (Ed.). The Quinolones, third ed., Academic Press, San Diego, (2000).
[3] Hooper,-DC; Rubinstein,-E (Eds.), Quinolone Antimicrobial Agents, third ed., ASM Press, Washington, DC, (2003).
[4] Turel,-I. Coord. Chem. Rev., 232: 27-47 (2002), and references cited therein.
[5] King,-DE; Malone,-R; Lilley,-SH. Am. Fam. Physician, 61: 2741–2748 (2000).
[6] Efthimiadou,-EK; Katsarou,-ME; Karaliota,-A; Psomas,-G. J. Inorg. Biochem. 102, 910-920 (2008).
[7] Belal,-F; Al-Majed,-AA; Al-Obaid,-AM. Talanta, 50: 765-786 (1999).
[8] Kapetanovi,-V; Milovanovi,-LJ; Erceg,-M. Talanta 43: 2123-2130 (1996).
[9] Rizk,-MS; Belal,-F; Ibrahim,-FA; Ahmed,-SM; Sheribah,-ZA. Electroanal., 12: 531-534 (2000).
[10] Zhang,-N; Zhang,-X; Zhao,-Y. Talanta, 62: 1041-1045 (2004).
[11] Zhang,-N; Zhang,-X; Zhao,-Y. Microchem. J. 75: 249-254 (2003).
[12] Turel,-I; Bukovec,-N; Farkas,-E. Polyhedron, 15: 269-275 (1996).
[13] Corboba-Diaz,-M; Cordoba-Borrego,-D.; Cordoba-Diaz, D. J. Pharm. Biomed. Anal. 18: 565-571 (1998).
[14] Rodriguez Cruz,-MS; Gonzalez Alonso,-I; Sanchez-Navarro,-A; Sayaler Marinero,-ML. Pharm Acta Helv., 73: 237-245 (1999).
[15] Sissi,-C; Andreolli,-M; Cecchetti,-V; Fravolini,-A; Gatto,-B; Palumbo,-M. Bioorg.Med.Chem, 6: 1551-1561 (1998).
[16] Efthimiadou,-EK; Katsarou,-M; Sanakis,-Y; Raptopoulou,-CP; Karaliota,-A; Katsaros,-N; Psomas,-G. J. Inorg. Biochem. 100: 1378-1388 (2006).
[17] Efthimiadou,-EK; Sanakis,-Y; Raptopoulou,-CP; Karaliota,-A; Katsaros,-N; Psomas,-G. Bioorg. Med. Chem. Lett. 16: 3864-3867 (2006).
[18] Efthimiadou,-EK; Thomadaki,-H; Sanakis,-Y; Raptopoulou,-CP; Katsaros,-N; Scorilas,-A; Karaliota,-A; Psomas,-G. J. Inorg. Biochem. 101: 64-76 (2007).
[19] Efthimiadou,-EK; Sanakis,-Y; Katsaros,-N; Karaliota,-A; Psomas,-G. Polyhedron, 26: 1148-1158 (2007).
[20] Efthimiadou,,-EK; Katsaros,-N; Karaliota,-A; Psomas,-G. Bioorg. Med. Chem. Lett.,17: 1238-1242 (2007).
[21] Tarushi,-A; P. Christo?s,-P; G. Psomas,-G. Polyhedron, 26: 3963-3972 (2007).
[22] Efthimiadou,-EK; Katsaros,-N; Karaliota,-A; Psomas,-G. Inorg. Chim. Acta 360: 4093-4102 (2007).
[23] Efthimiadou,-EK; Karaliota,-A; Psomas,-G. Polyhedron 27: 349-356 (2008).
[24] Katsarou,-ME; Efthimiadou,-EK; Psomas,-G; Karaliota,-A; Vourloumis,-D. J. Med. Chem. 51: 470-478 (2008).
[25] Mohamed,-GG; Abd El-Halim,-HF; El-Dessouky,-MMI; Mahmoud,-WH. J. Mol. Str., 999: 29-38 (2011).
[26] Abd El-Halim,-HF; Mohamed,-GG; El-Dessouky,-MMI; Mahmoud,-WH. Spectrochim. Acta (part A), 82: 8-19 (2011).
[27] Sakiyan,-I; Logoglu,-E; Arslan,-S; Sari,-N. Bio. Met. 17: 115-120 (2004).
[28] Skehan,-P; Storeng,-R. J. Natl. Cancer Inst. 42: 1107-1112 (1990).
[29] Cotton,-FA; Wilkinson,-G; Murillo,-CA; Bochmann,-M. Advanced Inorganic Chemistry, 6th edn., Wiley, New York, (1999).
[30] Abd El-halim,-HF; Omar,-MM; Mohamed,-GG; Sayed,-MA. Eur. J. Chem. 2: 178-188 (2011).
[31] Abd El-halim,-HF; Omar,-MM; Mohamed,-GG. Spectrochim. Acta (Part A), 78: 36-44 (2011).
[32] Abd-Elzaher,-MM. J. Chin. Chem. Soc. 48: 153-158 (2001).
[33] Mohamed,-GG; El-Gamel,-NEA. Spectrochim. Acta (Part A) 60: 3141-3154 (2004).
[34] Ali,-MA; Majumder,-SMMH; Butcher,-RJ; Jasinski,-JP; Jasinski,-JM. Polyhedron, 16: 2749-2754 (1997).
[35] Mohamed,-GG; Soliman,-MH. Spectrochim. Acta (Part A), 76: 341-347 (2010).
[36] Refat,-MS; Mohamed,-GG. J. Chem. Eng. Data., 55: 3239-3246 (2010).

[37] Sakai,-M; Hara,-A; Anjo,-A; Nakamura,-M. J. Pharm. Biomed. Anal., 18: 1057-1067 (1999).
[38] Jackman,-LM; Sternhell,-S. Applications of Nuclear Magnetic Resonance Spectroscopy in Organic Chemistry, Pergamon Press, Oxford, (1969).
[39] Freeman,-ES; Carroll,-B. J. Phys. Chem., 62: 397-397 (1958).
[40] Coats,-AW; Redfern,-JP. Nature, 201: 68-69 (1964).
[41] Horowitz,-HW; MJetzger,-G. Anal. Chem., 35: 1464-1468 (1963).
[42] Kandil,-SS; El-Hefnawy,-GB; Baker,-EA. Thermochim. Acta, 414: 105-113 (2004).
[43] Wallis,-SC; Gahan,-LR; Charles,-BG; Hambley,-TW. Aust. J. Chem., 47: 799-806 (1994).
[44] Turel,-I; Gruber,-K; Leban,-I; Bukovec,-N. J. Inorg. Biochem. 61: 197-212 (1996).
[45] Czugler,-M; Argay,-G; Frank,-J; Me´sza´ros,-Z; Kutschabsky,-L; Reck,-G. Acta Crystallogr. B 32: 3124-3126 (1976).
[46] Cygler,-M; Huber,-CP. Acta Crystallogr.C, 41: 1052-1055 (1985).
[47] Riley,-CM; Ross,-DL; Velde,-DV; Takusagawa,-F. J. Pharm. Biomed. Anal., 11: 49-59 (1993).
[48] Golic,-V; Sustar,-B; Barbo,-M. Joint Slovenian-Croatian Crystallographic Meeting. Oto?cec Book of Abstracts, p. 25 (1992).
[49] Florence,-AJ; Kennedy,-AR; Shankland,-N; Wright,-E; Al-Rubayi,-A. Acta Crystallogr. C 56: 1372 (2000).
[50] Turel,-I; Bukovec,-P; Quiro´s,-M. Int. J. Pharm. 152: 59-65 (1997).
[51] Sivalakshmidevi,-A; Vyas,-K; Om Reddy,-G. Acta Crystallogr. C56: e155-e116 (2000).
[52] Khan,-H; Badshah,-A; Murtaz,-G; Said,-M; Rehman,-Z; Neuhausen,-C; Todorova,-M; Jean-Claude,-B; Butler,-I. Eur. J. Med., 46: 4071-4077 (2011).
[53] Neelakantan,-MA; Esakkiammal,-M; Mariappan,-SS; Dharmaraja,-J; Jeyakumar,-T. Indian J. Pharm. Sci., 72: 216-222 (2010).
[54] Spratt,-TE; Schultz,-SS; Levy,-DE; Chen,-D; Schluter,-G; Williams,-GM. Chem. Res. Toxicol. 12: 809-815 (1999).
[55] Stass,-H; Kubitza,-D. Clin. Pharmacokinet, 40: 57-62 (2001).
[56] Alaghaz,-NMA; Ammar,-RA. Eur. J. Med. Chem. 45: 1314-1322 (2010).
[57] Prescott,-LM; Harley,-JP; Klein,-DA. Microbiology, 2nd ed. Wm. C. Brown Communications, Inc. (1993).

Source of support: Nil, Conflict of interest: None Declared